Biochimica et Biophysica Acta xxx (2013) xxx–xxx

Contents lists available at SciVerse ScienceDirect

Biochimica et Biophysica Acta

journal homepage: www.elsevier.com/locate/bbapap

H-bonding networks of the distal residues and water molecules in the active site of *Thermobifida fusca* hemoglobin ☆

Francesco P. Nicoletti [a], Enrica Droghetti [a], Barry D. Howes [a], Juan P. Bustamante [b], Alessandra Bonamore [c], Natascia Sciamanna [c], Darío A. Estrin [b], Alessandro Feis [a], Alberto Boffi [c], Giulietta Smulevich [a,*]

[a] *Dipartimento di Chimica "Ugo Schiff", Università di Firenze, Via della Lastruccia 3-13, I-50019 Sesto Fiorentino (FI), Italy*
[b] *Departamento de Química Inorganica, Analítica y Química Física/INQUIMAE-CONICET, Facultad de Ciencias Exactas y Naturales, Universidad de Buenos Aires, Ciudad Universitaria, Pabellon II, Buenos Aires C1428EHA, Argentina*
[c] *Institute Pasteur, Fondazione Cenci Bolognetti, Department of Biochemical Sciences and CNR, Institute of Molecular Biology and Pathology, University of Rome "La Sapienza", Piazzale Aldo Moro 5, I-00185 Rome, Italy*

ARTICLE INFO

Article history:
Received 10 January 2013
Received in revised form 19 February 2013
Accepted 22 February 2013
Available online xxxx

Keywords:
Hydroxyl ligand
Cyanide ligand
Hydrogen-bond
Resonance Raman
Truncated hemoglobin

ABSTRACT

The ferric form of truncated hemoglobin II from *Thermobifida fusca* (Tf-trHb) and its triple mutant WG8F-YB10F-YCD1F at neutral and alkaline pH, and in the presence of CN^- have been characterized by resonance Raman spectroscopy, electron paramagnetic resonance spectroscopy, and molecular dynamics simulations. Tf-trHb contains three polar residues in the distal site, namely TrpG8, TyrCD1 and TyrB10. Whereas TrpG8 can act as a potential hydrogen-bond donor, the tyrosines can act as donors or acceptors. Ligand binding in heme-containing proteins is determined by a number of factors, including the nature and conformation of the distal residues and their capability to stabilize the heme-bound ligand via hydrogen-bonding and electrostatic interactions. Since both the RR Fe–OH^- and Fe–CN^- frequencies are very sensitive to the distal environment, detailed information on structural variations has been obtained. The hydroxyl ligand binds only the WT protein giving rise to two different conformers. In form 1 the anion is stabilized by H-bonds with TrpG8, TyrCD1 and a water molecule, in turn H-bonded to TyrB10. In form 2, H-bonding with TyrCD1 is mediated by a water molecule. Unlike the OH^- ligand, CN^- binds both WT and the triple mutant giving rise to two forms with similar spectroscopic characteristics. The overall results clearly indicate that H-bonding interactions both with distal residues and water molecules are important structural determinants in the active site of Tf-trHb. This article is part of a Special Issue entitled: Oxygen Binding and Sensing Proteins.

1. Introduction

Ligand binding in heme-containing proteins is determined by a number of factors, including the nature and conformation of the distal residues and their capability to stabilize the heme-bound ligand via hydrogen-bonding and electrostatic interactions. The truncated hemoglobin II from *Thermobifida fusca* (Tf-trHb) contains three polar residues in the distal site: TrpG8, TyrCD1 and TyrB10. Whereas TrpG8 can act as a potential hydrogen-bond donor, the tyrosines can act as donors or acceptors.

The ferric and ferrous derivatives of truncated hemoglobins, analogous to mammalian globins, bind a variety of small molecules, such as H_2O, NO, CN^-, F^-, and CO. Previous studies carried out on the CO [1], F^- [2,3] and HS^- [4] adducts formed with the native Tf-trHb and a combinatorial set of mutants, in which the three distal amino acids have been singly, doubly, or triply replaced by a Phe residue, revealed that all the ligands are stabilized by TrpG8 via a strong H-bond. TyrCD1 is able to interact with CO and fluoride, whereas TyrB10 is not directly involved in ligand stabilization and plays only a minor role.

In the present work we have extended the analysis to the ferric form, studying the behavior of the ferric native protein and its triple mutant WG8F-YB10F-YCD1F at neutral and alkaline pH, and in the presence of CN^-. Since both the RR Fe–OH^- and Fe–CN^- frequencies are very sensitive to the distal environment, detailed information on structural variations can be obtained. In particular, the comparison of the spectroscopic signature of the OH^- ligated proteins at alkaline pH with those of the cyanide adducts is expected to provide information

Abbreviations: trHb, truncated hemoglobin; Tf, *Thermobifida fusca*; Hb, hemoglobin; WT, wild type; ASV, acidic surface variant of Tf-trHb containing two single site mutations Phe107Glu and Arg91Glu; Mb, myoglobin; MES, 2-(N-morpholino)ethanesulfonic acid; MD, molecular dynamics; EPR, electron paramagnetic resonance; RR, resonance Raman; 5c, five-coordinate; 6c, six-coordinate; HS, high spin; LS, low spin

☆ This article is part of a Special Issue entitled: Oxygen Binding and Sensing Proteins.

* Corresponding author. Tel.: +39 055 457 3083; fax: +39 055 457 3077.
E-mail address: giulietta.smulevich@unifi.it (G. Smulevich).

1570-9639/$ – see front matter © 2013 Elsevier B.V. All rights reserved.
http://dx.doi.org/10.1016/j.bbapap.2013.02.033

on the effects of H-bond interactions between the ligand and the distal residues as well on the Fe–CN geometry.

2. Material and methods

2.1. Sample preparation

Wild type (WT) Tf-trHb was expressed as a recombinant protein in *Escherichia coli* cells and purified as described previously [5]. As previously reported [1] the acidic surface variant (ASV) of Tf-trHb differs from the WT protein by mutation of both Phe107 and Arg91 to glutamic acid, which increases protein solubility during recombinant expression, without affecting thermostability or ligand binding properties [1–3]. Therefore, ASV was taken as an engineered scaffold of the WT protein for subsequent site-directed mutagenesis studies on the relevant residues of the distal heme pocket.

Phosphate salts and glycine were obtained from Merck AG (Darmstadt, Germany). 2-[N-morpholino]ethanesulfonic acid (MES) was bought from Sigma-Aldrich (Steinheim, Germany). All chemicals were of analytical or reagent grade and were used without further purification. The cyanide complexes were prepared by adding a few microliters of a diluted solution of potassium cyanide to the ferric proteins (ASV and triple mutant). Buffered solutions (0.1 M) were used for experiments at pH 9.8–10.1 (glycine), 7.0 (phosphate), and 6.1 (MES).

Protein concentrations in the range 10–70 μM were used for the electronic absorption and RR samples. Sample concentration for low-temperature RR was between 30 and 100 μM. Sample concentrations for electron paramagnetic resonance (EPR) experiments were in the range 130–600 μM.

The protein concentration was determined on the CO derivative in the presence of 10–20 mM sodium dithionite by using an extinction coefficient of 174000 M^{-1} cm^{-1} for Tf-trHb.

2.2. Spectroscopic characterization

Electronic absorption spectra, measured with a double-beam spectrophotometer (Varian Cary 5), were recorded using a 1 cm quartz cuvette and a 600 nm/min scan rate. Absorption spectra (using a 5-mm NMR tube) were measured both prior to and after RR measurements to ensure that no degradation had taken place under the experimental conditions used. RR spectra were measured with excitation at 413.1 nm (Kr^+ laser, Coherent, Innova 300C) using a triple spectrometer (consisting of two Acton Research SpectraPro 2300i working in the subtractive mode, and a SpectraPro 2500i in the final stage with a 3600 grooves/mm grating), equipped with a liquid-nitrogen cooled CCD detector (Roper Scientific Princeton Instruments). RR spectra were calibrated with indene, n-pentane, and carbon tetrachloride as standards to an accuracy of 1 cm^{-1} for intense isolated bands.

The low-temperature experiments were carried out using an Air Products Displex closed-cycle He refrigerator with automatic temperature control. For the low-temperature RR measurements, 20 μL of the protein solution was deposited on the copper cold finger of the refrigerator at 90 K under a nitrogen flow. The temperature was then slowly decreased to 12 K under vacuum, and RR spectra were obtained at this temperature.

All RR measurements were repeated several times under the same conditions to ensure reproducibility. To improve the signal-to-noise ratio, a number of spectra were accumulated and summed only if no spectral differences were noted. All spectra were baseline corrected. To determine peak bandwidth and positions, a curve-fitting program (Lab Calc; Galactic) was used to simulate the spectra using a Lorentzian line shape. The frequencies of the bands were optimized with an accuracy of 1 cm^{-1}, and the bandwidths with an accuracy of 0.5 cm^{-1}. Bandwidths (full width at half-maximum) varied as follows: 12–14 cm^{-1} in the high frequency region; 9–12 cm^{-1} for the low frequency region.

EPR spectra were recorded as reported previously [6] and the g-values were determined by careful visual inspection of the spectra.

2.3. Molecular dynamics simulations

The simulations were performed starting from the crystal structure of WT Tf-trHb determined at 2.48 Å resolution, Protein Data Bank (PDB) entry 2BMM [5]. Two different systems of protein-ligand complexes, with a water or hydroxide ligand bound to the heme group, were built and simulated. The water molecule was added in the distal site bound to Fe(III) according to the equilibrium structure in an isolated model system QM calculation at the DFT level (with the PBE functional and 6–31 G** basis sets), taking into account the distal site environment. The charges and parameters for Fe(III) heme — water molecule were determined by a standard procedure: partial charges were computed using the restricted electrostatic potential (RESP) recipe and DFT electronic structure calculations with the PBE functional and 6–31 G** basis sets. The calculation has been performed in the high spin (HS) state. Equilibrium distances and angles, as well as force constants, were computed using the same methods and basis set used for computed charges. The same procedure was used for the hydroxide ligand. The parm99 force field implemented in AMBER was used to describe the protein [7]. The system was then immersed in a pre-equilibrated octahedral box of 4909 TIP3P water molecules using the tLEaP module of the AMBER package [7]. We used periodic boundary conditions with a 9 Å cutoff and Ewald sums for treating long-range electrostatic interactions. The SHAKE algorithm [8] was used to keep bonds involving H atoms at their equilibrium length, allowing us to use a 2 fs time step for the integration of Newton's equations. The histidine tautomeric state and protonation (Nε–H, Nδ–H, His^+) were carefully analyzed for each of the three His residues (namely His99, His122, and His135) and set to favor the hydrogen bond network suggested by the experimental crystal structure. Equilibration protocol consisted of (i) slowly heating the whole system from 0 to 300 K for 20 ps at constant volume, with harmonic restraints of 80 Kcal per mol A^2 for all Cα atoms; (ii) pressure equilibration of the entire system simulated for 1 ns at 300 K with the same restrained atoms. After these two steps unconstrained 30 ns of molecular dynamics (MD) simulations at constant temperature (300 K) were performed. To simulate the triple mutant (YB10F-YCD1F-WG8F) protein, we introduced in silico mutations by changing the corresponding amino acid in the original structure and allowing the system to equilibrate as mentioned earlier. All structures were found to be stable during the timescale of the simulations, as evidenced by the root mean square displacements (RMSD), depicted in Fig. S1, Supplementary data.

3. Results

3.1. Hydroxyl ligand

Fig. 1 shows the UV–vis titration and the RR spectra in the high frequency region of Tf-trHb between pH 6.1 and 10.1, together with the corresponding spectra of the triple mutant at neutral pH. In this pH range Tf-trHb undergoes coordination and spin state changes. At acidic pH the absorption spectrum shows a Soret band at 407 nm (409 nm at neutral pH), Q bands at 498, 541 and 577 nm, and a broad CT band centered at 634 nm. The corresponding RR spectrum clearly indicates that at low pH the protein is a mixture of three species, an aquo 6cHS (ν_3 at 1480 cm^{-1}, ν_2 at 1563 cm^{-1}), a 6cLS (ν_3 at 1503 cm^{-1}, ν_2 at 1579 cm^{-1}, ν_{10} at 1638 cm^{-1}) and a small amount of 5cHS form (ν_3 at 1489 cm^{-1} and ν_2 at 1570 cm^{-1}). At alkaline pH the 5cHS species disappears, and, similar to Hb and Mb [9], the absorption spectrum becomes typical of a hydroxo complex characterized by a mixture of 6cHS and 6cLS species with the Soret band at 413 nm, Q bands at 545 and 577 nm, and a shoulder at about 609 nm due to the CT1 band. Accordingly, at alkaline pH, in the high frequency RR region two sets of core size marker bands are found, corresponding to a

Please cite this article as: F.P. Nicoletti, et al., H-bonding networks of the distal residues and water molecules in the active site of *Thermobifida fusca* hemoglobin, Biochim. Biophys. Acta (2013), http://dx.doi.org/10.1016/j.bbapap.2013.02.033

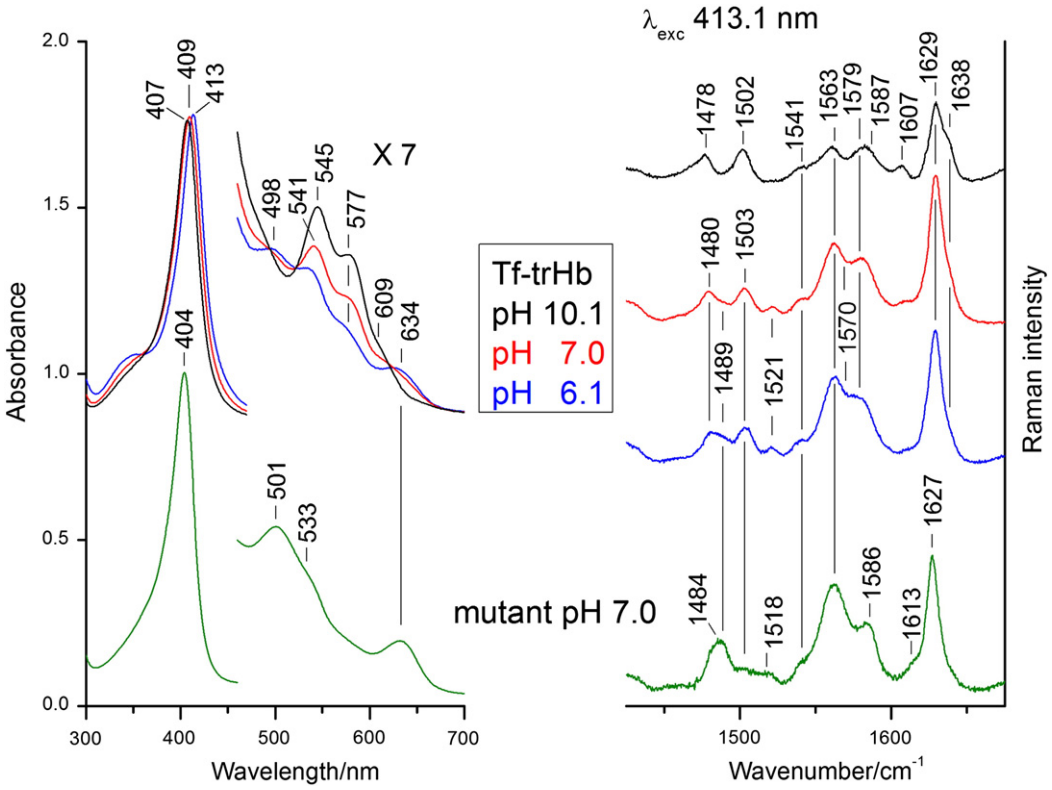

Fig. 1. UV–Vis titration (left) and RR spectra (right) in the high frequency region of Tf-trHb at pH 6.1, 7.0, and 10.1, together with the corresponding spectra of the triple YB10F-YCD1F-WG8F mutant at neutral pH. Left: the region between 460 nm and 700 nm has been expanded seven-fold. Right: 413.1 nm laser excitation; 1 cm^{-1} spectral resolution. Experimental conditions: Tf-trHb: 10 mW laser power at the sample; average of 3 spectra (pH 6.1 and 7.0) and 2 spectra (pH 10.1) with 240 s integration time; Triple mutant: 15 mW laser power at the sample; average of 3 spectra with 360 s integration time. A baseline has been subtracted from all spectra. Spectra have been shifted along the ordinate axis to allow better visualization.

hydroxo 6cHS (ν_3 at 1478 cm^{-1}, ν_2 at 1563 cm^{-1}, ν_{37} at 1587 cm^{-1}) and 6cLS (ν_3 at 1502 cm^{-1}, ν_2 at 1579 cm^{-1}, ν_{37} at 1607 cm^{-1}, ν_{10} at 1638 cm^{-1}). The two forms, existing in a thermal spin-state equilibrium at room temperature, convert to almost a pure 6cLS heme at 15 K (ν_3 at 1506 cm^{-1}, ν_2 at 1588 cm^{-1}, ν_{10} at 1642 cm^{-1}) (Fig. S2, Supplementary data). The triple mutant behaves quite differently. Between pH 6.1 and 7.0 the absorption spectrum does not change (data not shown) and it is mainly characteristic of an HS form with the Soret band at 404 nm, Q bands at 501 and 533 nm, and CT at 634 nm; the corresponding RR spectrum clearly indicates the presence of a predominant 6cHS species (ν_3 at 1484 cm^{-1}, ν_2 at 1563 cm^{-1}, ν_{37} at 1586 cm^{-1}, ν_{10} at 1613 cm^{-1}). The broadness of the ν_3 band suggests also the presence of a 5cHS, which has been confirmed by a band fitting analysis which clearly shows ν_3 at 1489 cm^{-1}, and ν_2 at 1567 cm^{-1} (data not shown). In addition, a weak ν_3 at 1503 cm^{-1} is observed due to a 6cLS species. At alkaline pH the protein becomes unstable.

Fig. 2 (left) shows the low frequency region RR spectra of Tf-trHb at alkaline pH in H_2O, D_2O, and $H_2^{18}O$ buffered solutions, at 298 and 15 K, together with the corresponding band fitting analysis. Table 1 reports the band fitting parameters together with the band assignments. Whereas the hydroxide 6cHS complex is present at room temperature and undetectable at 15 K, at both temperatures the band at 485 cm^{-1} is affected by the isotopic substitution. It up-shifts by 4 cm^{-1} in D_2O (489 cm^{-1}), and downshifts to 471 cm^{-1} (−14 cm^{-1}) in $H_2^{18}O$, as also confirmed by the difference spectra (Fig. 2, right). Therefore, the band at 485 cm^{-1} is assigned to the ν(Fe–OH) stretching mode of the 6cLS form. Hence, in Tf-trHb the low-spin ν(Fe–OH) stretching mode is about 65 cm^{-1} lower than the corresponding bands observed for metMb and metHb [9]. This anomalous very low frequency indicates unusually strong hydrogen bonding between the OH^- ligand and distal residues. In fact, with an increase of the H-bond strength, a decrease of the force constant of the Fe–OH bond together with a loss of its biatomic oscillator character (via vibrational coupling with the Fe–OH bending and torsion and the O–HX stretch modes) is expected. In addition, the strength of the H-bond is predicted to weaken upon deuterium substitution; in particular, for O···O distances > 2.6 Å [10]. As a consequence, the Fe–OD stretch can experience a smaller downshift, or even an upshift, compared with the corresponding Fe–OH stretch despite the increased mass.

Fig. 3 shows the EPR spectra (at 5 K) at alkaline and neutral pH of the Tf-trHb and its triple mutant. On the basis of previously reported hydroxo complexes (Table 2), the LS species with g_1 values in the range g = 2.7–2.8 are assigned to His/OH coordination, where the OH group is strongly H-bonded. The weak species with g_1 = 2.66 is similar to cases of His/OH coordination where the OH group is not strongly H-bonded. The g-values and assignments of the various Tf-trHb LS species are reported in Table 2.

At pH 6, the HS signal for both samples becomes considerably more intense than that observed for WT at alkaline pH, whereas the LS signals are approximately 10-fold weaker compared to the LS species of WT at alkaline pH. The inset (Fig. 3) shows the relative intensities of the LS signals of the three spectra (without expansion), clearly demonstrating the marked intensification of the LS signals at alkaline pH. At pH 6 all the high spin bands show a variable degree of rhombicity. This suggests that the HS state is a 5c species or, alternatively, there is a mixture of 6cHS and 5cHS species present. The apparently lower $g_\perp$ value in the case of the WT HS signal (5.71) compared to that of the mutant (5.85) is probably simply due to the superposition of a more rhombic 5cHS and a 6cHS species. The extremely weak HS signal at alkaline pH is characterized by a rhombic g tensor (6.31, 5.85, 1.99) (data not shown), and likely results from free heme dissociated from the protein due to structural instability at alkaline pH.

Classical MD simulations of Fe(III) Tf-trHb with coordinated water were performed to shed light on the nature of the H-bond network

Please cite this article as: F.P. Nicoletti, et al., H-bonding networks of the distal residues and water molecules in the active site of *Thermobifida fusca* hemoglobin, Biochim. Biophys. Acta (2013), http://dx.doi.org/10.1016/j.bbapap.2013.02.033

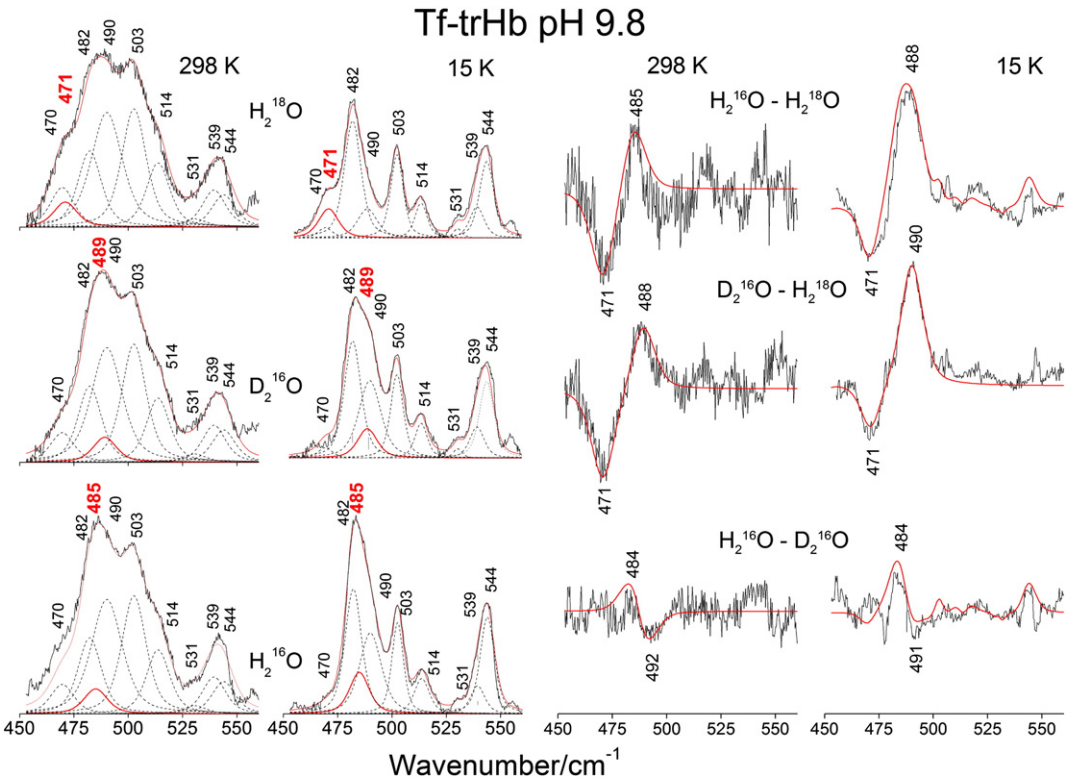

Fig. 2. (Left) Low-frequency region RR spectra of alkaline Tf-trHb, pH 9.8 or pD 10.0, at 298 K and 15 K, obtained in H_2O, D_2O, and $H_2^{18}O$. Experimental conditions: 1 cm^{-1} spectral resolution; 10 mW (298 K) and 12 mW (15 K) laser power at the sample; average of 5 spectra with 600 s integration time. Red lines indicate the total curve-fitted spectra (see Material and methods). The individual fitting components are displayed as dashed lines, except for the ν(Fe–OH) component (red continuous line). The frequency of the ν(Fe–OH) stretching mode (bold red character) is highlighted. (Right) Difference RR spectra obtained from the experimental (black line) and fitted (red line) spectra on the right-hand side of the figure.

stabilizing the coordinated water molecule, as suggested by the spectroscopy data. At neutral pH, the calculations were performed on the HS state as identified by the spectroscopic measurements. In agreement with the experimental results, the optimized Fe–OH_2 bond distance was found to be about 2.2–2.3 Å for both proteins. We found that in both the WT and the triple mutant the coordinated water is stabilized by H-bonds. However, in agreement with the spectroscopic data, the strength of the H-bonds in the two cases is quite different. In the WT protein the water is strongly H-bonded with the indole N proton of the WG8 (H_2O — N_{WG8} = 1.9 Å) and the hydroxylic hydrogen of the YCD1 (O_{H2O} — O_{YCD1} = 1.5 Å) (Fig. 4A) justifies the spectroscopic finding of an Fe–OH^- character of the ligand even at pH 6.1. On the contrary, in the triple mutant YB10F-YCD1F-WG8F the ligand maintains the characteristics of a water molecule. In fact, the mutant was able to accommodate three water molecules close to the active site (Fig. 4B). To characterize the internal water interactions, we evaluated the radial distribution function g(r) for the O atom of the water molecules, centered on the coordinated water for the last 30 ns of the simulation. The integration of the g(r) function confirmed the presence of two water molecules around the distal ligand interacting weakly via H-bonds (see Fig. 4B, $O_{H2O}(W1) - O_{H2O}(W2) = 2.8$ Å; $O_{H2O}(W2) - O_{H2O}(W3) = 3$ Å).

Table 1
Band fitting parameters and band assignment in the low frequency region.[a]

RR frequency (cm^{-1})	Bandwidth (cm^{-1})	Mode assignment
470		
485 (+4; −14)	11	ν(Fe-OH)
Theor. (−15; −24)		
482	9	ν_{33} B_{2g}
490	12	γ_{22} E_g
503	9	γ_{12} B_{1u}
514	9	ν_{25} A_{2g}
531	9	ν_{49} E_u
539	9	γ_{21} E_g
544	9	ν_{48} E_u

[a] In brackets is reported the isotopic shift in D_2O and $H_2^{18}O$, respectively.

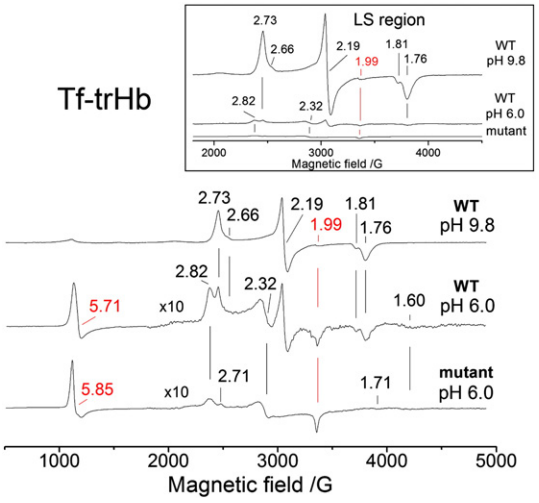

Fig. 3. X-band EPR spectra of WT Tf-trHb at pH 9.8 in 0.1 M glycine and pH 6.0 in 0.1 M MES and its triple mutant (WG8F-YB10F-YCD1F) at pH 6.0. The g-values of the HS and LS species are shown in red and black, respectively. The inset shows the relative intensities of the LS signals of the three spectra (without expansion), clearly demonstrating the marked intensification of the LS signals at alkaline pH. The spectra were recorded at 5 K, 10 G modulation amplitude and 0.01 mW (WT) and 1.0 mW (mutant) microwave power. The spectra have been shifted along the ordinate axis to allow better visualization.

Please cite this article as: F.P. Nicoletti, et al., H-bonding networks of the distal residues and water molecules in the active site of *Thermobifida fusca* hemoglobin, Biochim. Biophys. Acta (2013), http://dx.doi.org/10.1016/j.bbapap.2013.02.033

Table 2
EPR spectral parameters of WT Tf-trHb, its triple mutant and various low-spin hydroxide bound (His-Fe-OH^-) heme proteins.

Protein	LS signals					HS signals		REF
	g_1	g_2	g_3	Intensity[a]	Coordination	$g_\perp$	$g_{\|\|}$	
WT Tf-trHb pH 9.8	2.73	2.19	1.76	s	His/OH^{-b}			This work
	2.66	2.19	1.81	vw	His/OH^-			This work
WT Tf-trHb pH 6.0	2.82	2.32	1.60	vw	His/OH^{-b}	5.71	1.99	This work
	2.73	2.19	1.76	vw	His/OH^{-b}			This work
	2.66	2.19	1.81	vvw	His/OH^-			This work
Mutant of Tf-trHb pH 6.0	2.82	2.32	1.60	vvw	His/OH^{-b}	5.85	1.99	This work
	2.71	–	1.71	vvw	His/OH^{-b}			
HRPA2[c]	2.96	2.13	1.66		His/OH^{-b}			[25]
Mb	2.55	2.17	1.85		His/OH^-			[26]
Lucina pectinata Hb II	2.61	2.20	1.82		His/OH^-			[26]

[a] s, strong; w, weak; vvw, extremely weak.
[b] OH^- strongly H-bonded.
[c] HRPA2, Horseradish peroxidase isoenzyme A2.

At alkaline pH, two different conformers were found for the WT protein during the timescale of the MD simulation. Fig. 5 displays the change of the H-bonding distance between OH^- and O_{YCD1} as a function of time, showing the interconversion of conformers, as well as a representation of the distal side in both conformations. The optimized Fe–OH bond distance was found to be about 1.8 Å. In both forms the hydroxide ligand is strongly stabilized by three H-bonds involving the distal polar residues. In one form, TrpG8 and TyrCD1 directly interact with the ligand ($OH - N_{WG8} = 3.1$ Å; $OH - O_{YCD1} = 3.2$ Å), whereas TyrB10 is H-bonded to a water molecule which, in turn, is H-bonded with the distal ligand ($OH^- - H_2O(W1) = 2.7$ Å; $H_2O(W1) - O_{YB10} = 2.6$ Å) (Fig. 5A). In the second conformer only the TrpG8 is directly H-bonded with the hydroxide ($OH - N_{WG8} = 3.1$ Å), whereas both the tyrosines interact with the ligand via a water molecule ($OH^- - H_2O(W2) - O_{YCD1}$ = both 2.6 Å; $OH^- - H_2O(W1) - O_{YB10} = 2.7$ and 2.6 Å) (Fig. 5B).

3.2. Cyanide ligand

Upon addition of cyanide to both WT and the triple mutant, their sixth ligand is replaced by the exogenous ligand to form a cyanide 6cLS complex. Both UV–vis (419, 543, 578 nm) and RR spectra in the high frequency region (ν_3 at 1503 cm^{-1}, ν_2 at 1582 cm^{-1}, ν_{10} at 1637 cm^{-1}) are identical to each other and similar to other cyanide complexes (data not shown).

Figs. 6 and 7 show the low-frequency RR spectra of the cyanide adducts of ferric Tf-trHb and its triple variant, respectively, along with those of the $^{13}C^{14}N$, $^{12}C^{15}N$, and $^{13}C^{15}N$ analogs to effectively identify those modes associated with the Fe(III)-CN linkage. It is immediately apparent that for the Tf-trHb the band at 439 cm^{-1} exhibits a monotonic downshift as the mass of cyanide increases from $^{12}C^{14}N$ (439 cm^{-1}), through $^{13}C^{14}N$ and $^{12}C^{15}N$ (436 cm^{-1}), to $^{13}C^{15}N$ (432 cm^{-1}). Therefore, this band is assigned to the ν(FeCN) mode. The isotope-sensitive mode at 380 cm^{-1} exhibits a zigzag isotope shift pattern. The difference spectra show features at about 383 and 378 cm^{-1}. Since the zigzag pattern is characteristic of a bending mode [11], we assign the band at 380 cm^{-1} to the δ(Fe–C–N) mode. Accordingly, this band disappears in the difference spectra obtained by subtraction of pairs of the spectra of adducts in which the mass of the carbon atoms is equal but the total mass of the cyanide isotopomers is different ($^{12}C^{14}N$-$^{12}C^{15}N$ and $^{13}C^{14}N$-$^{13}C^{15}N$). In fact, in these two cases, the bending vibrations should occur at the same frequency and thus cancel out, whereas features associated with the stretching modes should appear in the difference spectra.

Inspection of Fig. 6 reveals the presence of several weak isotope-sensitive bands which are not readily discernable in the RR spectra owing to their weak intensity, but clearly appear in the difference spectra. In the region near 420 cm^{-1} another band shows a zigzag pattern, with difference maxima appearing at 415–419 cm^{-1} and minima at 405–407 cm^{-1}. Simulated difference spectra (Fig. S3, Supplementary data) indicate that this corresponds to a band with

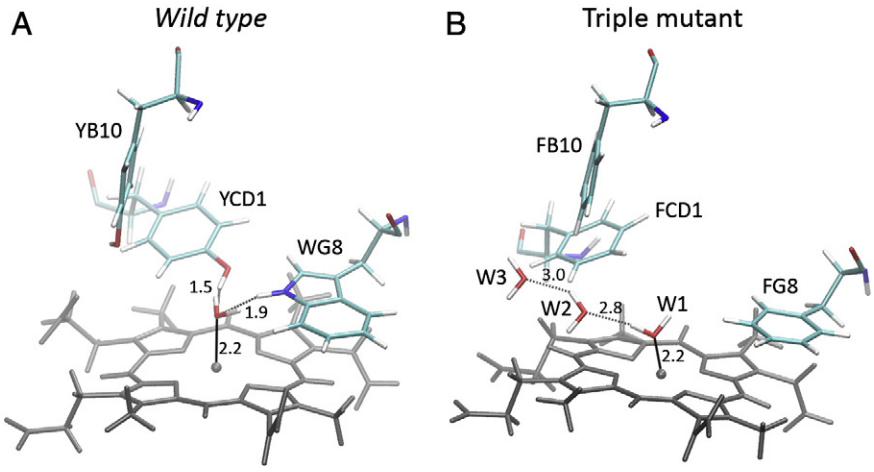

Fig. 4. Schematic representation of the distal side of WT Tf-trHb (A) and its TrpG8F-TyrB10F-TyrCD1F triple mutant (B), showing the hydrogen-bond network (dotted lines) stabilizing the iron-bound H_2O on the basis of MD simulations. Distances are in angstroms.

Please cite this article as: F.P. Nicoletti, et al., H-bonding networks of the distal residues and water molecules in the active site of *Thermobifida fusca* hemoglobin, Biochim. Biophys. Acta (2013), http://dx.doi.org/10.1016/j.bbapap.2013.02.033

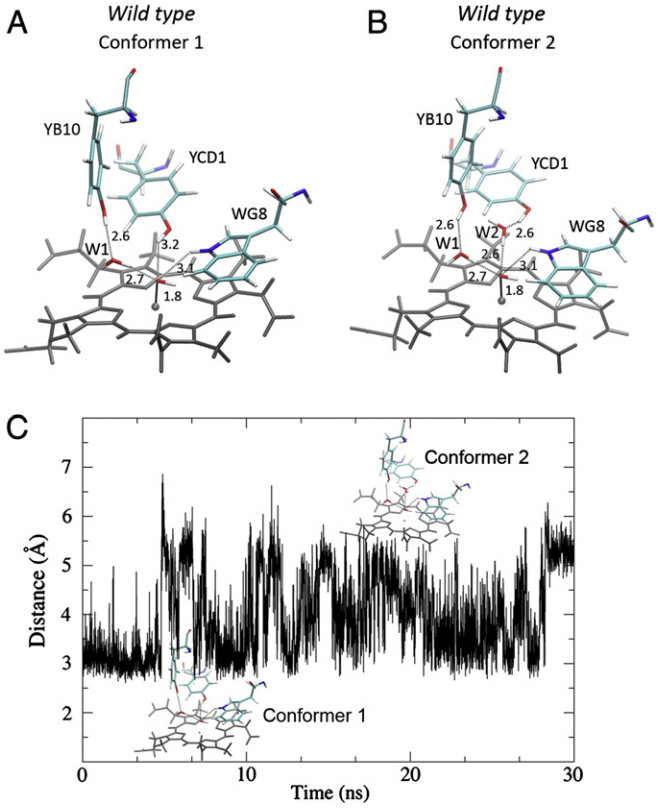

Fig. 5. (A and B): Schematic representation of the distal side of the two conformers of the WT Tf-trHb at alkaline pH showing the hydrogen-bond network (dotted lines) stabilizing the iron-bound OH^- on the basis of MD simulations. Distances are in angstroms. (C): Time evolution of OH-O_{YCD1} distance showing swapping configurations between two conformers during the timescale of simulation.

maximum at 414 cm^{-1} in the natural isotopomer spectrum and full width at half maximum 20 cm^{-1}.

The intensity pattern in the difference spectra is closely related to that of the 380 cm^{-1} band. In addition, as for the band at 380 cm^{-1}, this band disappears in the difference spectra obtained by subtraction of pairs of the spectra of adducts in which the mass of the carbon atoms is equal but the total mass of the cyanide isotopomers is different ($^{13}C^{14}N$-$^{13}C^{15}N$) and ($^{12}C^{14}N$-$^{12}C^{15}N$) and is observed, together the band at 380 cm^{-1}, in the difference spectra ($^{12}C^{15}N$-$^{13}C^{14}N$) where only the bending modes are present. Therefore, we assign this band as another δ(Fe–C–N) mode, similar to the RR spectra of cyanide adducts of horseradish peroxidase at pH 12 [12], which displayed a secondary δ(Fe–C–N) band at 420 cm^{-1} with a ν(Fe–CN) band at 355 cm^{-1}. The corresponding ν(Fe–CN) cannot be identified in our spectra, however, we cannot rule out that it is obscured by the intense porphyrin ν_8 band at 347 cm^{-1}. However, the RR results provide unambiguous evidence that a main CN conformer has been found, exhibiting ν[Fe–CN] and δ[Fe–C–N] modes at 439 and 380 cm^{-1}.

The effect of the distal residue mutations is small (Fig. 7). The main change in the RR spectra of the CN^- adduct of the TrpG8Phe-TyrCD1Phe-TyrB10-Phe triple mutant is a shift of the δ[Fe–C–N] band from 380 to 370 cm^{-1}, together with a 7 cm^{-1} shift of the secondary δ[Fe–C–N] band. The intensity changes in the difference spectra follow a pattern which is similar to that of the native protein.

4. Discussion

Extensive work on heme proteins has demonstrated that the frequency of the ν(Fe–OH) RR mode depends on the Fe ion spin state, the distal environment, and especially on the number and strength of H-bonding interactions between the hydroxide and the distal polar residues. [9,13–15]. Typical ν(Fe–OH) wavenumbers are around 490 and 550 cm^{-1} for 6cHS and 6cLS species, respectively. H-bonding can lower the stretching frequency by decreasing the Fe–O electron density and, as a consequence, the Fe–OH force constant. For example, in horseradish peroxidase only a 6cLS form has been found at 503 cm^{-1}, as the hydroxide is stabilized by accepting H-bonds from the distal His and the distal Arg. Similarly for Tf-trHb, only the 6cLS species has been identified. It is characterized by an extremely low ν(Fe–OH) frequency, about 65 cm^{-1} lower than the corresponding vibration in Mb. This frequency strongly supports the presence of numerous H-bonds formed by the bound hydroxyl with distal residues and water molecules. Based on MD simulations, the OH^- anion builds three H-bonds in alkaline Tf-trHb form1 with TrpG8 and TyrCD1 (which is fully consistent with the results obtained with other ligands, see below), and with a water molecule H-bonded to TyrB10. In form 2, H-bonding with TyrCD1 is mediated by a water molecule.

Previous studies carried out on the CO [1], F^- [2,3], and HS^- [4] adducts formed with the WT protein and a combinatorial set of mutants, in which these three amino acids have been singly, doubly, or triply replaced by a Phe residue, revealed that all the ligands are stabilized by TrpG8 via a strong H-bond. TyrCD1 is able to interact with CO and fluoride, whereas TyrB10 is not directly involved in the ligand stabilization and plays only a minor role. Therefore, the present case is the first example of involvement of TyrB10 – albeit an indirect one – in the stabilization of the exogenous ligand. In fact, previously we found that in the presence of the fluoride anionic ligand, which can only accept H-bonds, TrpG8 and TyrCD1 form strong H-bonds with fluoride since the WT protein is characterized by a ν(Fe–F) stretch at 385 cm^{-1}. In contrast, the YB10F-YCD1F-WG8F mutant displayed the highest ν(Fe–F) stretch (471 cm^{-1}). These results clearly highlight that the heme environment, where fluoride is surrounded by three Phe residues, does not appear to be apolar as would be expected. Accordingly, MD simulations indicated that two water molecules, interacting with the coordinated fluoride ion, are accommodated in the active site. Unlike fluoride, hydroxide can act as an H-bond donor or acceptor. In addition, whereas TrpG8 can act as a potential hydrogen-bond donor only, the tyrosines can act as donor or acceptor. Therefore, we suggest that in the present case whereas TrpG8 and TyrCD1 stabilize the hydroxide by donating a proton, similar to the fluoride case, TyrB10 acts as an H-bond acceptor. In fact, crystallographic data indicate that the TyrCD1 phenol hydroxide is directed toward the hydrogen bond coordination sphere of the iron bound ligand, whereas the TyrB10 phenol hydroxide is clearly directed “off axis” in the direction of the heme propionate, with respect to the ligand. It is thus envisaged that the phenolic oxygen atom of TyrB10 may assume a conformation that is favorable for a hydrogen bond acceptor.

Whereas the ν(Fe–OH) mode is very sensitive to the nature of the distal residues, its frequency being markedly affected by the presence of H-bonds between the oxygen and polar residues, the RR frequencies of the CN conformers may be interpreted in terms of steric hindrances within the distal cavity. A CN^- anion in the absence of any steric hindrance should bind to a ferric heme with a linear (upright) geometry. In this case the δ[Fe–C–N] mode should be RR-inactive. However, deviations from linearity are possible and, in fact, are occasionally observed in the X-ray structures of cyanide complexes of heme proteins. Accordingly, the observed ν[Fe–CN] and δ[Fe–C–N] Raman frequencies are significantly scattered since sterically encumbering groups in close contact with the bound CN^- cause a bent Fe–CN unit and a decrease of the Fe–CN stretching frequency [16].

The Fe–CN stretching frequency in various hemoproteins typically falls in the 400–460 cm^{-1} range. For instance, the ν[Fe–CN] RR bands of MbCN and HbCN were observed around 452 cm^{-1} [17], which corresponds to a slightly bent FeCN moiety [18]. In fact, the ν[Fe–CN] of an unhindered CN-bound heme complex was observed at 456 cm^{-1}, whereas analogous “strapped hemes”, in which the ligand binding is

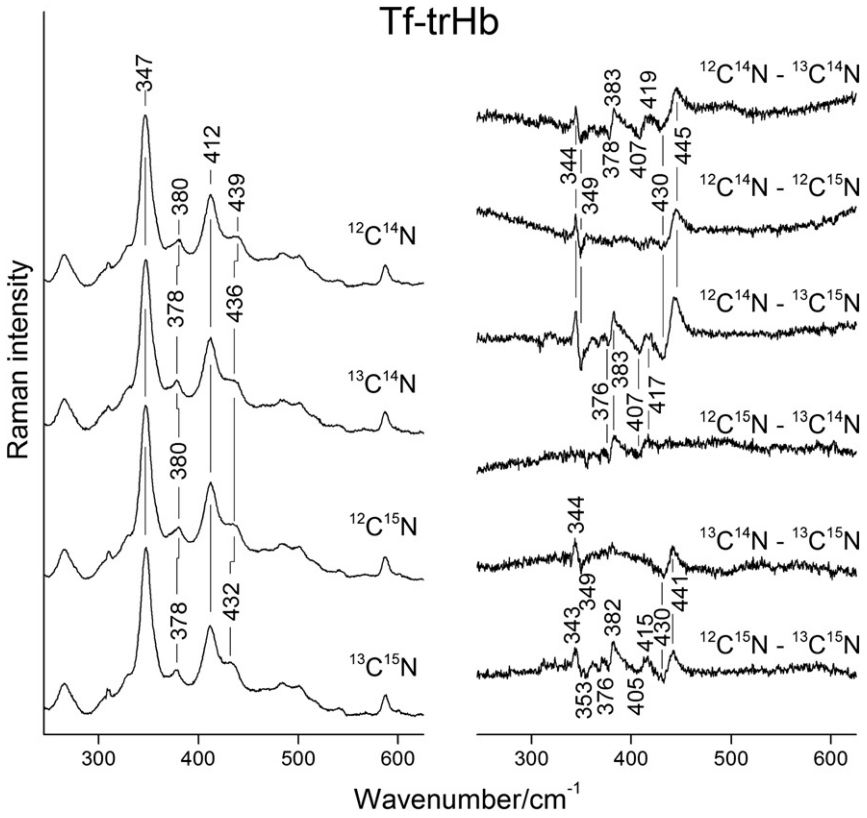

Fig. 6. Left: low-frequency region RR spectra of the cyanide complexes of ferric Tf-trHb for the four isotopes at pH 7.0; right: difference spectra. Experimental conditions: 1 cm^{-1} spectral resolution; 10 mW laser power at the sample. $^{12}C^{14}N$, average of 11 spectra; $^{12}C^{15}N$, average of 6 spectra; $^{13}C^{14}N$, average of 6 spectra; $^{13}C^{15}N$, average of 5 spectra. Integration time for each spectrum was 1200 s.

sterically hindered by a $(CH_2)n$-chain strap over the iron at the CN^- binding site, displayed downshifted ν[Fe–CN] frequencies, i.e. between 447 and 445 cm^{-1} for n between 15 and 13 [16].

In the present case, for both proteins we observe a main conformer characterized by ν[Fe–CN] at about 440 cm^{-1}, more than 10 cm^{-1} lower than that of mammalian globins, with a smaller isotopic shift (7 cm^{-1}) than the expected value for a linear Fe–CN oscillator, and a δ[Fe–C–N] at 380 cm^{-1} (370 cm^{-1} in the mutated protein). Therefore, we propose that the Fe–C–N moiety adopts a bent structure similar to other truncated hemoglobins [19–21] which is maintained in the triple mutant, where the polar residues are replaced by the non-polar Phe. A second, less abundant conformer, is characterized by a δ[Fe–C–N] band frequency at 414 cm^{-1} (407 cm^{-1} in the mutant) whose corresponding ν[Fe–CN] has not been clearly observed, and likely has an even less linear Fe–CN moiety. In fact, on the basis of normal-mode calculations [12,22] it has been proposed that for the linear or slightly bent conformers the Fe – CN stretching mode has a frequency higher than the bending mode, whereas the strongly bent conformer exhibits a reverse pattern in which the frequency of the bending mode is higher than that of the stretching mode.

Similar results have been obtained for the CN adduct of the single domain Hb from *Campylobacter jejuni*. The two conformers have been assigned to a "linear" Fe–C–N moiety (ν[Fe–CN] at 440 cm^{-1} and δ[Fe–C–N] at 403 cm^{-1}) and a "bent" form (ν[Fe–CN] at 353 cm^{-1} and δ[Fe–C–N] at 417 cm^{-1}) [23]. The corresponding X-ray structure (2WY4) indeed shows an almost linear Fe–CN unit (176^0) with a strong H-bond between the cyanide ion and the TyrB10 residue.

A combination of RR and X-ray data of cyanide complexes of truncated bacterial heme proteins is available only for *Chlamydomonas eugametos* trHb. In the wild-type protein, the highly constrained structure of the Fe–C–N moiety is a result of distal interactions. In fact, the ν(Fe–CN) at 440 cm^{-1} in the native protein shifts up to 452 cm^{-1} in the GlnE7Gly mutant, consistent with a more relaxed structure in the mutant. Conversely, when the TyrB10 is mutated to Leu, the ν(Fe–CN) frequency shifts down to 435 cm^{-1}, indicating an even more constrained structure [19]. We found a somewhat related situation in a mutated plant hemoglobin from *Arabidopsis thaliana*. In that case, the ν(Fe–CN) frequency for the complex of the native protein was at 454 cm^{-1}. Mutation of the distal Phe residue to Leu induced a downshift to 439 cm^{-1}, possibly due to an increased steric hindrance, whereas the distal His to Leu mutation lead to a ν(Fe–CN) at 457 cm^{-1}, corresponding to an unhindered FeCN moiety [24].

We finally note that the similarity of the RR results obtained for native Tf-trHb and the triple mutant suggests that H-bonding interactions with the cyanide ligand have negligible effects. However, distal H-bonding with water molecules may be present in the mutant as well, similar to the case of the fluoride adduct [3]. Preliminary MD simulations on the WT and the triple mutant indicate that in both cases the CN^- ligand is strongly H-bonded. In the native protein the H-bonds are donated by the TrpG8 and TyrCD1 residues, whereas in the triple mutant, two water molecules interacting with the coordinated cyanide ion are accommodated into the active site (data not shown).

5. Conclusions and perspectives

In conclusion, we have demonstrated how complementary structural information can be obtained by a combination of RR spectra, EPR spectra and MD simulations of the cyanide and hydroxide complexes of Tf-trHb. Whereas the effect of distal H-bonding on the ν(Fe–OH) band has been rationalized, further studies are necessary to highlight the correlation between RR Fe–CN frequencies, X-ray structures, and MD simulations, taking into account the effect of both steric effects and H-bonding interactions.

Please cite this article as: F.P. Nicoletti, et al., H-bonding networks of the distal residues and water molecules in the active site of *Thermobifida fusca* hemoglobin, Biochim. Biophys. Acta (2013), http://dx.doi.org/10.1016/j.bbapap.2013.02.033

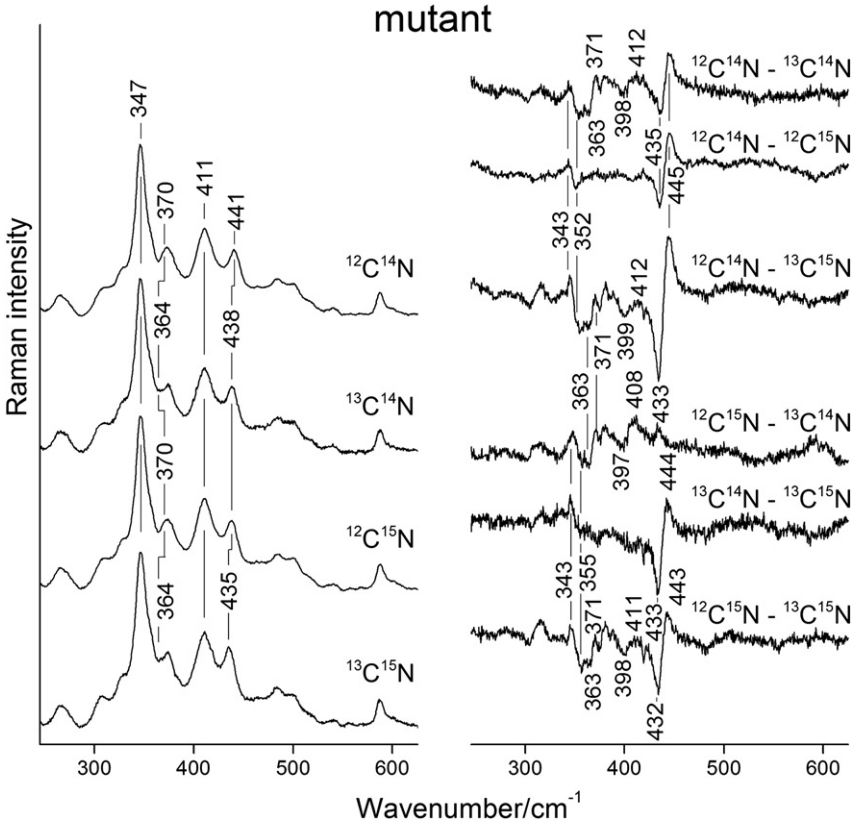

Fig. 7. Left: low-frequency region RR spectra of the cyanide complexes of the ferric triple variant for the four isotopes at pH 7.0; right: difference spectra. Experimental conditions: 1 cm^{-1} spectral resolution; 10 mW laser power at the sample. $^{12}C^{14}N$, average of 17 spectra; $^{12}C^{15}N$, average of 19 spectra; $^{13}C^{14}N$, average of 3 spectra; $^{13}C^{15}N$, average of 8 spectra. Integration time for each spectrum was 1200 s.

Acknowledgments

This work was supported by the Institute Pasteur Fondazione Cenci Bolognetti (A. Boffi), MIUR FIRB RBFR08F41U_002 (A. Bonamore), MIUR PRIN 2008BFj34 (A. Feis and A. Boffi), University of Buenos Aires (grant X074), CONICET and European Union FP7 project NOStress (D. Estrin), and the Italian Ministero dell'Istruzione, dell'Università e della Ricerca (MIUR), Direzione Generale per l'Internazionalizzazione della Ricerca, Progetti di Grande Rilevanza Italia-Argentina. We thank Dr Maria Fittipaldi for provision of EPR facilities and assistance in recording the spectra.

Appendix A. Supplementary data

Supplementary data to this article can be found online at http://dx.doi.org/10.1016/j.bbapap.2013.02.033.

References

[1] E. Droghetti, F.P. Nicoletti, A. Bonamore, L. Boechi, P. Arroyo Manez, D.A. Estrin, A. Boffi, G. Smulevich, A. Feis, Heme pocket structural properties of a bacterial truncated hemoglobin from *Thermobifida fusca*, Biochemistry 49 (2010) 10394–10402.
[2] E. Droghetti, F.P. Nicoletti, A. Bonamore, N. Sciamanna, A. Boffi, A. Feis, G. Smulevich, The optical spectra of fluoride complexes can effectively probe H-bonding interactions in the distal cavity of heme proteins, J. Inorg. Biochem. 105 (2011) 1338–1343.
[3] F.P. Nicoletti, E. Droghetti, L. Boechi, A. Bonamore, N. Sciamanna, D.A. Estrin, A. Feis, A. Boffi, G. Smulevich, Fluoride as a probe for H-bonding interactions in the active site of heme proteins: the case of *Thermobifida fusca* Hemoglobin, J. Am. Chem. Soc. 133 (2011) 20970–20980.
[4] F.P. Nicoletti, A. Comandini, A. Bonamore, L. Boechi, F.M. Boubeta, A. Feis, G. Smulevich, A. Boffi, Sulfide binding properties of truncated hemoglobins, Biochemistry 49 (2010) 2269–2278.
[5] A. Bonamore, A. Ilari, L. Giangiacomo, A. Bellelli, V. Morea, A. Boffi, A novel thermostable hemoglobin from the actinobacterium *Thermobifida fusca*, FEBS J. 272 (2005) 4189–4201.
[6] F.P. Nicoletti, M. Thompson, B.D. Howes, S. Franzen, G. Smulevich, New insights into the role of distal histidine flexibility in ligand stabilization of dehaloperoxidase-hemoglobin from *Amphitrite ornate*, Biochemistry 49 (2010) 1903–1912.
[7] D.A. Pearlman, D.A. Case, J.W. Caldwell, W.S. Ross, T.E. Cheatham III, S. DeBolt, D. Ferguson, G. Seibel, P. Kollman, AMBER, a package of computer programs for applying molecular mechanics, normal mode analysis, molecular dynamics and free energy calculations to simulate the structural and energetic properties of molecules, Comput. Phys. Commun. 91 (1995) 1–41.
[8] J.-P. Ryckaert, G. Ciccotti, H.J.C. Berendsen, Numerical integration of the cartesian equations of motion of a system with constraints: molecular dynamics of n-alkanes, J. Comput. Phys. 23 (1977) 327–341.
[9] A. Feis, M.P. Marzocchi, M. Paoli, G. Smulevich, Spin state and axial ligand bonding in the hydroxide complexes of metmyoglobin, methemoglobin, and horseradish peroxidase at room and low temperatures, Biochemistry 33 (1994) 4577–4583.
[10] T. Saitoh, K. Mori, R. Itoh, Two-dimensional vibrational analysis of the Lippincott-Schröder potential for OH – O, NH – O and NH – N hydrogen bonds and the deuterium isotope effect, Chem. Phys. 60 (1982) 161–180.
[11] N.-T. Yu, B. Benko, E.A. Kerr, K. Gersonde, Iron-carbon bond lengths in carbonmonoxy and cyanomet complexes of the monomeric haemoglobin III from *Chironomus thummi thummi*: a critical comparison between resonance Raman and X-ray diffraction studies, Proc. Natl. Acad. Sci. U. S. A. 81 (1984) 5106–5110.
[12] J. Al-Mustafa, J.R. Kincaid, Resonance Raman study of cyanide-ligated horseradish peroxidase. Detection of two binding geometries and direct evidence for the "push-pull" effect, Biochemistry 33 (1994) 2191–2197.
[13] B.D. Howes, J.N. Rodriguez-Lopez, A.T. Smith, G. Smulevich, Mutation of distal residues of horseradish peroxidase: influence on substrate binding and cavity properties, Biochemistry 36 (1997) 1532–1543.
[14] G.S. Lukat-Rodgers, K.R. Rodgers, Spin-state equilibria and axial ligand bonding in FixL hydroxide: a resonance Raman study, J. Biol. Inorg. Chem. 3 (1998) 274–281.
[15] T. Egawa, S.-R. Yeh, Structural and functional properties of hemoglobins from unicellular organisms as revealed by resonance Raman spectroscopy, J. Inorg. Biochem. 99 (2005) 72–96.
[16] T. Tanaka, N.T. Yu, C.K. Chang, Resonance Raman studies of sterically hindered cyanomet "strapped" hemes. Effects of ligand distortion and base tension on iron-carbon bond, Biophys. J. 52 (1987) 801–805.

[17] S. Hirota, T. Ogura, K. Shinzawa-Itoh, S. Yoshikawa, T. Kitagawa, Observation of multiple CN-isotope-sensitive Raman bands for CN^- adducts of hemoglobin, myoglobin, and cytochrome c oxidase: evidence for vibrational coupling between the Fe-C-N bending and porphyrin in-plane modes, J. Phys. Chem. 100 (1996) 15274–15279.
[18] M. Bolognesi, C. Rosano, R. Losso, A. Borassi, M. Rizzi, J.B. Wittenberg, A. Boffi, P. Ascenzi, Cyanide binding to *Lucina pectinata* hemoglobin I and to sperm whale myoglobin: an X-Ray crystallographic study, Biophys. J. 77 (1999) 1093–1099.
[19] T.K. Das, M. Couture, M. Guertin, D.L. Rousseau, Distal interactions in the cyanide complex of ferric *Chlamydomonas* haemoglobin, J. Phys. Chem. B 104 (2000) 10750–10756.
[20] M. Milani, A. Pesce, Y. Ouellet, P. Ascenzi, M. Guertin, M. Bolognesi, *Mycobacterium tuberculosis* haemoglobin N displays a protein tunnel suited for O_2 diffusion to the heme, EMBO J. 20 (2001) 3902–3909.
[21] M. Milani, Y. Ouellet, H. Ouellet, M. Guertin, A. Boffi, G. Antonini, A. Bocedi, M. Mattu, M. Bolognesi, P. Ascenzi, Cyanide binding to truncated hemoglobins: a crystallographic and kinetic study, Biochemistry 43 (2004) 5213–5221.
[22] J. Al-Mustafa, M. Sykora, J.R. Kincaid, Resonance Raman investigation of cyanide ligated beef liver and *Aspergillus niger* catalases, J. Biol. Chem. 270 (1995) 10449–10460.
[23] C. Lu, M. Mukai, Y. Lin, G. Wu, R.K. Poole, S.-R. Yeh, Structural and functional properties of a single domain hemoglobin from the food-borne pathogen *Campylobactor jejuni*, J. Biol. Chem. 282 (2007) 25917–25928.
[24] F. Spyrakis, S. Faggiano, S. Abbruzzetti, P. Dominici, E. Cacciatori, A. Astegno, E. Droghetti, A. Feis, G. Smulevich, S. Bruno, A. Mozzarelli, P. Cozzini, C. Viappiani, A. Bidon-Chanal, F.J. Luque, Histidine E7 dynamics modulates ligand exchange between distal pocket and solvent in AHb1 from *Arabidopsis thaliana*, J. Phys. Chem. B 115 (2011) 4138–4146.
[25] B.D. Howes, A. Feis, C. Indiani, M.P. Marzocchi, G. Smulevich, Formation of two types of low-spin heme in horseradish peroxidase isoenzyme A2 at low temperature, J. Biol. Inorg. Chem. 5 (2000) 227–235.
[26] D.W. Kraus, J.B. Wittenberg, J.F. Lu, J. Peisach, Hemoglobins of the *Lucina pectinata*/Bacteria Symbiosis, J. Biol. Chem. 265 (1990) 16054–16059.

Please cite this article as: F.P. Nicoletti, et al., H-bonding networks of the distal residues and water molecules in the active site of *Thermobifida fusca* hemoglobin, Biochim. Biophys. Acta (2013), http://dx.doi.org/10.1016/j.bbapap.2013.02.033